

## **Coupled Flow Network Model and CFD Analysis for a Combined Impingement and Film Cooled Gas Turbine Nozzle Guide Vane**

Pol Reddy Kukutla, B.V.S.S.S Prasad

Thermal Turbomachines Laboratory, Department of Mechanical Engineering,  
Indian Institute of Technology Madras, Chennai-36, India.

### **Abstract**

The nozzle guide vane (NGV) of a gas turbine engine possesses complex cooling passages, with inherent thermo-fluid dynamic interactions between the vane and the main stream. The present paper is an attempt to make use of the Computational Fluid Dynamics(CFD) tools as well as the flow network analysis tools, in combination, for analyzing typical cooled NGV flow passages. CFD results containing the static and total pressure contours are presented in the paper and are summarized as simple correlating relations; these in turn are used to generate the discharge coefficients as input to the flow network. The pressure conditions at different boundary nodes are further input to the flow network analysis. The mass flow rate and pressure drop values through the impingement and film holes are obtained as output from the flow network model. Comparison of the results from one-dimensional approach coupled with three- dimensional CFD analysis with the available literature by Jin et al. [7] shows a good agreement for the operating pressure ratio in the range of 1.2 to 1.5 at pressure surface rows of the film cooling holes in the leading edge region of the vane. The accuracy of the calculated total pressure ratio on the pressure surface rows of the leading edge circuit has been found satisfactory. The coolant from FIT and AIT are 25.5% and 74.5% respectively. The secondary fluid flows from FIT is 24.3% fed to the leading edge film holes, while 51.9% of coolant is fed to the mid-chord region through the film holes, 22.5% coolant flows out of the trailing edge film holes and the remaining 1.3% flows through trailing edge slot

### **Keywords**

CFD, Film Cooling, Flow Network Model, Jet impingement Cooling, Nozzle Guide Vane.

## 1. Introduction

In the preliminary design stage of a cooled gas turbine nozzle guide vane (NGV), two-dimensional numerical methods are not very appropriate. On the other hand, both three-dimensional analyses of NGV cooling passages and the experimental techniques are very time-consuming, as their geometries are too complex with multiple rows of (inline/staggered) impingement and film holes. The conventional approach to analyzing flows in such sophisticated passages is to use the one-dimensional network method, with short turnaround time, sufficient accuracy, and limited effort. Making use of experimental information as input such network models help the design of optimum internal cooling configurations for the NGV.

Probably the first classical work on simulation of gas turbine vane cooling flow networks was reported by Damerow et al [1]. They developed flow models representative of leading edge impingement, mid-chord cooling; pin fins, feeder supply tube, and a composite model of a complete airfoil flow system were tested. Test conditions were set by varying pressure level to cover the Mach number and Reynolds number range of interest in advanced turbine applications. Selected geometrical variations were studied on each component model to determine these effects. Orifice flow was correlated in terms of discharge coefficients. The coefficients obtained were incorporated into a compressible flow network analysis computer program, which was developed to predict the flow distribution in the complex turbine blade cooling configurations. Results using this program compared favorably with experimental result from the composite model, which simulated an actual turbine airfoil cooling system incorporating the individual components.

Jen and Sobanik et al [2] developed an analytical model for the prediction of cooling air flow characteristics such as mass flow rate and internal pressure distribution in the gas turbine components. They addressed a number of basic flow elements such as orifices, frictional passages, seals etc. They also introduced the concept of equivalent pressure ratio to account for the centrifugal effect in rotating condition. They obtained the data from static bench test and measured the total coolant flow rate. Both were in good agreement with the analysis at different pressure ratio.

A generalized one-dimensional code for analyzing the flow and heat transfer in turbomachinery cooling passages was presented by Ganesh et al. [3].

Numerical procedure to design internal cooling of gas turbine stator blades was proposed by Carcasci and Facchini [4] using the networks of different cooling systems.

Martin and Dulikravich [5] reported a computer program based on 1D in-house code COOLNET for the thermo-fluid flow network analysis in order to predict coolant flow rates, total

coolant pressures, bulk coolant total temperatures, and internal heat transfer coefficient distributions of a rotor blade which is used by Pratt and Whitney.

Rama Kumar and Prasad [6] developed 1D in-house code NETSOLVER with combined CFD and network approach to simulate turbine blade cooling system. They simulated the turbine blade as a circular cylinder. CFD was used to compute the loss coefficients (K factors) and thermal resistances. These resistance values were fed to the 1D code and were simulated. The cooling system results indicate that increase in the coolant to mainstream flow ratio causes decrease in coolant exit temperature and hence increase in film cooling effectiveness.

A compressible 1D flow network model analysis was successfully developed by Jin et al. [7] for the root cause analysis of an aero derivative high pressure turbine rotor blade film cooling oxidation. It was found that the presence of an inlet metering plate at the blade root, combined with a larger total exit flow area of the aeroderivative design not only reduced the total cooling flow rate, altered the flow distribution but also reduced the internal pressure compared to its aero-engine design.

A multi-dimensional platform for heat transfer analysis of air-cooled turbine blades and vanes was introduced by Zhongran et al. [8]. They used 1D flow network model at the design level and 1D film cooling model for performance prediction. Detailed design level used conjugate heat transfer simulation of ANSYS CFX. The flow network solver with an integrated flow network model and film cooling model achieved stability by solving momentum equation in a linear method.

A decoupled procedure to predict cooling performances and metal temperatures of gas turbine blades and nozzles were presented by Andrei et al. [9]. Various inputs needed for the procedure were evaluated by different tools. Mainstream parameters were estimated by 3D CFD simulations while the blade internal cooling system was modeled by an in-house one-dimensional fluid network approach. The heat conduction through the solid was computed through a 3D FEM method. These methods were employed for a NASA-C3X internally film-cooled vane and the results were compared with the experimental data.

Yan et al. [10] investigated the combination of Flow Network Model (FNM) with conjugate heat transfer to improve the design of integrated cooling structures in a high-performance turbine blade, coupled with the 3D viscous solver for the gas flow field.

Tran and Kapat [11] performed an exact, closed-form analytical solution to the enhanced lumped capacitance model derived for the conduction in a representative two-dimensional ribbed surface for the case of perfect thermal contact. The modeled behavior of the coupled zero-

dimensional/one-dimensional model showed reasonable agreement with the numerical simulation.

Che et al. [12] made calculations for both steady and transient state problems by using the component method and network method toward series and parallel networks. They showed that the whole engine model simulated by the component method is suitable for observing the safety of engine influenced by the dynamic characteristic of the secondary air system

Angersbach and Bestle [13] described an automated preliminary aero-thermal design process for a rich burn combustor by combining preliminary design tool, 2D geometry model coupled with a 1D network solver in order to speed up the preliminary design loop and provide improved combustor designs. The 1D network solver then would calculate the air distribution inside the combustor for two different combustor cooling schemes. The computed air distribution was subsequently used to predict emissions which were minimized by using a genetic multi-objective optimization algorithm.

Suresh et al. [14] carried out 1D flow network approach using Flowmaster commercial software for the flow and conjugate heat transfer analysis to improve the durability analysis for internally cooled rotor blade to predict the coolant mass flow rate, bulk temperature, and pressure as a result of secondary air system which would affect the performance of turbine blade heat transfer. The 1D simulation values were validated against experimental data

A predictive model for the gas turbine blade cooling analysis using 1D network in-house code was developed by Chowdhury et al. [15] to predict the thermal loadings in the turbine vane/blade, It was necessary to conduct the overall analysis for a set of different boundary conditions with the same blade model (E3) and simulate the external hot gas flow condition, the conduction in the blade material, and the internal coolant flow characteristics accurately and simultaneously for the most efficient and advanced cooling system design. The simultaneous solutions resulted from the coupled equations of mass and energy balance. The 1D model was validated by showing its accuracy to predict the temperature distributions of a NASA E3 blade with an uncertainty of less than +/-10%. As a result, 1D model was proposed as a novel, quicker, and more convenient way for the overall analysis and for a set of different boundary conditions with the same blade (NASA E3)

Chandran and Prasad [16] carried out both the numerical and experimental studies on the leading edge region of a typical gas turbine NGV, cooled by a combination of impingement and showerhead film cooling. A detailed flow and conjugate heat transfer study revealed that the complex flow structure results owing to the coolant-mainstream interaction and the influence of vane material thermal conductivity.

Wang et al. [17] investigated on the vehicle underhood thermal management the core of the integrated vehicle thermal management. As the engine cooling, air conditioning turbocharged cooling, oil cooling and others were set in the under-hood, this approach was used to discuss the relevance of the multiple thermodynamic systems and the structure change. So the simulation approach coupling 1D simulation and 3D simulation was proposed to realize the comprehensive analysis. The 1D simulation was mainly about the relevance of systems and thermodynamic system cycles. The 3D simulation was mainly about the structural analysis. The MATLAB routine was used to compile the 1D model program and the combination module.

Pol Reddy and Prasad [18] numerically investigated the effect of various combinations of coolant mass flow rates and mainstream Reynolds number, supplied at the front and aft impingement cooling plenums subjected to three-dimensional conjugate heat transfer analysis for the combined impingement and film cooled gas turbine nozzle guide vane.

One of the most recent multipurpose analysis was carried out on the first stage stator-rotor turbine cavity of a heavy-duty gas turbine secondary air system by Bavassano et al. [19]. This involved steady 3D CFD calculations with a computational domain comprising the first turbine stage and the corresponding stator-rotor wheel space. A combined CFD and SASAC, the in-house Ansaldo 1D fluid network code, was used to adjust its internal pressure and consequently lower the global rotor axial load acting on the thrust bearing. This goal had to be reached while maintaining safety against hot gas ingestion from the turbine section main flow into the cavity, thus preserving the integrity of gas turbine. Two field measurement campaigns were subsequently carried out on an AE94.2 gas turbine to validate both the baseline configuration and the upgraded one by means of six pressure and temperature sensors in the cavity and twelve load cells/thermocouples on the thrust bearing. The CFD model and results were presented, the fluid network tuning was discussed and the experimental setup and its main outcomes for the two field campaigns were reported.

In most of the foregoing investigations, coupled 1D and 3D approaches pertaining to either internal cooling channels of the gas turbine blade with a single film cooled row or stator-rotor cavities are considered. In none of these investigations, details of individual flow rates from each row of film holes are reported for a combined impingement and film cooling configuration of the nozzle guide vane.

The present paper mainly focuses on bringing out the effect of spanwise coolant mass flow rate distribution and spanwise total pressure drop distribution at all the rows of both the impingement and film holes on the leading edge of the vane. Results of variation of mass flow

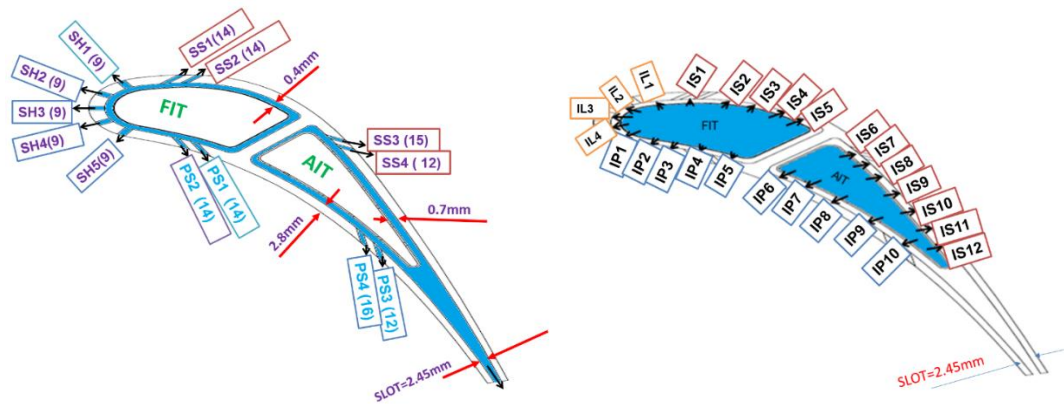
rate and pressure drop are presented at three sections from hub to tip of the nozzle guide vane surface.

## 2. Computational Methodology

### 2.1 Nozzle Guide Vane Geometry Details

The NGV for the present study is developed from the geometric details available for a high-pressure turbine vane. It comprises of (i) the outer surface of the NGV, divided into three parts: the leading edge, the pressure and the suction surfaces shown in Fig. 1(a) (ii) two impingement inserts: front impingement tube (FIT) and aft impingement tube (AIT) shown in Fig 1(b).

Figure.1 shows a view of the mid-section, consisting of these three parts of the leading edge, developed by extruding the mid-section profiles. There are a total of 156 number of film holes, distributed throughout the NGV outer surface and in thirteen rows of in-line arrangement. The FIT and AIT have 217 and 144 numbers of impingement holes respectively. The thickness of FIT is 0.4mm and that of AIT is 0.7mm. The gap between the impingement inserts and the rear side of the vane is 2.8mm throughout.



(a) NGV outer Surface with film holes marked (b) FIT and AIT with impingement holes marked

Fig. 1. Sectional view of Nozzle Guide Vane

The NGV is designed in such a way that the coolant enters the FIT and AIT inlets, passes through the impingement holes and hits the rear side of the NGV as small jets. After impingement, the coolant from the FIT effuses out of the five rows of holes arranged in the form of shower head at the leading edge. These rows are named as SH1 to SH5 in Fig 1(a), further, there are two rows of film holes (SS1 and SS2) on the suction side and two rows on pressure side (PS1 and PS2). The coolant that enters the AIT, after impingement, effuses out through the remaining film holes on the suction side (SS3 and SS4), pressure side (PS3 and PS4) and through the trailing edge slot of width 2.45mm.

## 2.2 Computational Domain

The computational domain consists of three zones:

Fluid Zone 1: Mainstream flow around the NGV.

Fluid Zone 2: Coolant flow through impingement inserts impingement holes, spacing between inserts and vane, and through the film holes.

Solid Zone3: Solid regions of the NGV that correspond to the thickness of the vane and inserts

All the edges and faces of the geometry model are cleaned and made suitable for very fine grid generation

## 2.3 Meshing

The mesh for computational study, as shown in Figure 3, is generated using commercial software Gambit 2.4.6. A hybrid mesh is generated in the fluid zones and solid zone mentioned in the previous section. For flow past turbine airfoils, direct resolution of the near wall flow is preferred instead of using wall functions to predict the boundary layer profiles. The near wall turbulence models require a low  $y^+$  value, say 2 or smaller, with a very refined mesh close to the vane surface. Hence, a three-dimensional boundary layer type mesh, as can be seen from figure 3, is provided on the vane surface where the interaction between the mainstream and the coolant has to be captured with high accuracy.

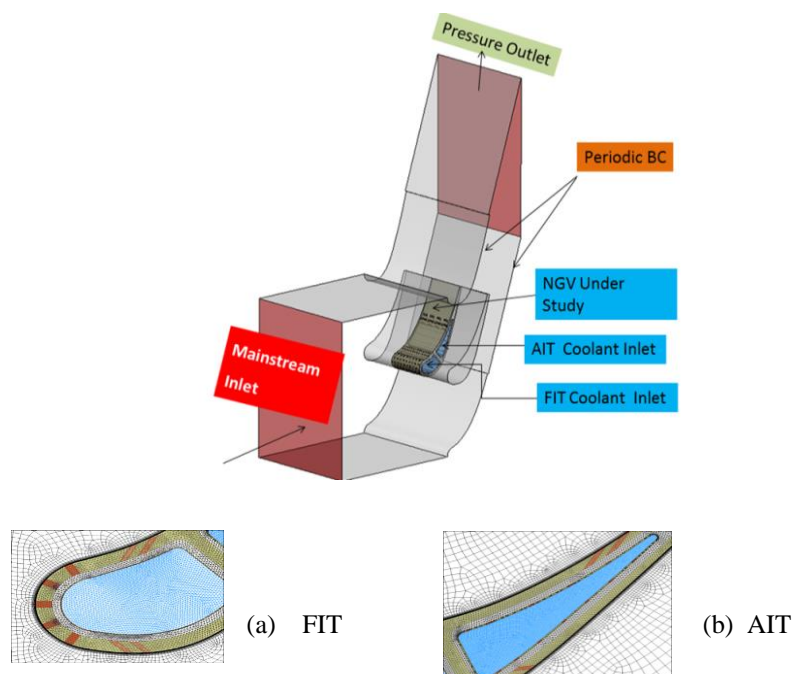


Fig. 2. Computational domain

## 2.4 Solution Methodology

The conservation equations necessary to be solved for simulation of the three-dimensional conjugate heat transfer problem are those of mass, momentum and energy. These equations are selected from Fluent 14.5 code, consistent with the assumptions of steady, incompressible, constant thermophysical property fluid with negligible viscous dissipation, radiation, and natural convection. The  $\kappa$ - $\omega$  SST (Shear Stress Transport) model is adopted for turbulence modeling.

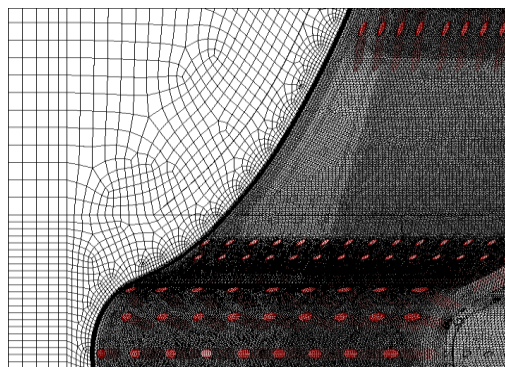


Fig. 3. Mesh in the region close to the NGV surface

### 2.4.1 Boundary Conditions

The other input conditions for the present study are: velocity inlet condition at the mainstream inlet, pressure outlet condition at mainstream outlet, mass flow inlet condition at front impingement tube (FIT) and aft impingement tube (AIT) coolant inlets, no-slip boundary condition at the wall, periodic boundary condition at the internal walls, conjugate thermal condition at the walls of the NGV and adiabatic boundary condition on the symmetry planes.

### 2.4.2 Grid Independence Study

Grid independence study is conducted with three mesh sizes: coarse, medium and fine; with details as given in Table 1. The coarse mesh has approximately 9.8 million cells and the wall  $y^+$  is close to 1.5. The medium and fine meshes has cells close to 12.7 million and 15.1 million respectively and their wall  $y^+$  values were improved to 0.8 and 0.5 respectively by further refining the near wall mesh. The spanwise averaged effectiveness at various streamwise locations of the vane was calculated and plotted in Figure 4. When the mesh is improved from coarse to medium, a maximum difference in the effectiveness value of about 3% is witnessed. Whereas a further refinement of mesh showed a maximum difference of less than 1% between medium and fine mesh effectiveness values. For a cost of 2.4 million cells, this difference is negligibly small. Hence, the medium mesh is found optimum and adopted for the present computational model. In



this mesh, a  $y^+$  value less than 0.8 is ensured throughout the vane surface and at the film holes exit by providing a three dimensional boundary layer with first row height of 0.02mm and a growth factor of 1.2 for 20 rows.

Table 1. Details of cells used for meshing

Mesh	No. of cells	Maximum $y^+$ Value
Coarse	9.8 million	1.5
Medium	12.7 million	0.8
Fine	15.1 million	0.5

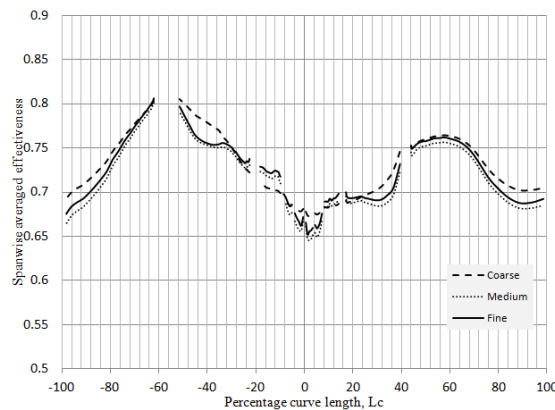


Fig. 4. Grid Independence Study

### 3. Flow Network Model

A numerical 1-D model was developed by using Flownex software to simulate thermo-fluid dynamic phenomena, consistent with these assumptions and inclusive of friction and heat transfer.

Flownex<sup>®</sup> 8.6.1. 2642, a 1-D commercial code is used for the cooling system analysis by means of a 1-D circuit scheme. In this method, the entire physical model is subdivided into several basic nodes and elements, to predict thermo-fluid-dynamic output conditions from a sub-system, using the given inlet conditions. The boundary conditions of the circuit are set at the beginning of the simulation through the specified amount of coolant flow rate, inconsistent with the CFD code.

The one-dimensional model approach consists of an element is essentially a control volume which represents the plenum chamber, impingement holes and film holes. The nodes represent the connection points between elements, which can be either reservoir or tank and hence the

nodes have been considered as multiple inlets and outlets with the properties within a node assumed to be homogeneous and represented by a single averaged value.

In the solution of the integrated network all the fluid volume, and therefore all the fluid mass, is assumed to be contained within the nodes, but the net change of momentum between all the inlets and outlets of a node is assumed to be negligible. Flownex<sup>®</sup>8.6.1.2642 software solves the conservation equations for the steady-state solution directly and quickly for the given set of boundary conditions.

### 3.1 Mass Conservation at a Node

The Fig. 5 shows the control volume with various number of inlets and exits. The fundamental mass conservation equation for each node is based on the analogy of Kirchhoff current law in electricity, which states that the mass flow into and out of the each node must be equal. The sign convention adopted for the node is the mass flow into the node will be considered as positive, while the mass flow leaving the node will be regarded as negative.

The spatially integrated steady partial differential form of a mass equation without internal sources that are solved for each node are given by

$$\sum_{j=1}^n \dot{m}_j = \sum_{e=1}^m \dot{m}_e \quad (1)$$

Where  $j=1, 2, 3$  and so on for 'n' inlets

and  $e=1, 2,$  and so on 'm' outlets.

Therefore, the sum of the mass flows equals to zero in the absence of an external mass addition or extraction to the node.

$$\sum_{j=1}^n S_{ij} \dot{m}_j = 0 \quad (2)$$

Where  $S_{ij}$  represents the sign of flow in element  $j$  relative to the node  $i$ , and the subscript  $j$  indicates the branch number.

$S_{ij} = -1$ , when fluid flows out from the node

$S_{ij} = +1$ , when fluid flows into the node.

$S_{ij} = 0$ , if element  $j$  has no connection with the node  $i$ .

Here  $n$  is the total number of nodes.

### 3.2 Momentum Equation for an Element

Pressure losses occurring at the inlets and outlets of the node volume should be lumped on the elements adjacent to the node. In this case, where the node acts as a junction, the algebraic sum of the head losses in any closed loop within the system must be zero.

The steady, one-dimensional, incompressible momentum conservation equation solved for each element in order to obtain the pressure difference across the each element is given by

$$p_i - p_e = \frac{K}{2} \rho V^2 \quad (3)$$

Where  $p$  is the total pressure,  $V$  the weighted average velocity in the control volume,  $\rho$  is the coolant density and  $K$  is the loss coefficient due to frictional losses which intern depends on the discharge coefficient of the hole respectively

### 3.3 Energy Equation at a Node

The conservation of energy for a finite control volume with one-dimensional inlets and outlets neglecting the body forces, then integral form of the equation is based on the the sum of the inward heat flow at a specified junction or node is equal to the sum of the outward heat flow at that specified junction is given by

$$\sum \dot{m}_i h_{0i} = \sum \dot{m}_e h_{0e} \quad (4)$$

The assumptions in the equation (4) is that there is no work done and heat transfer within the node. Here  $h_0$  is specific total enthalpy of the fluid,  $\dot{m}$  is the mass flow rate, and the average property values at the inlets and outlets are represented with the subscripts  $i$  and  $e$  refer respectively.

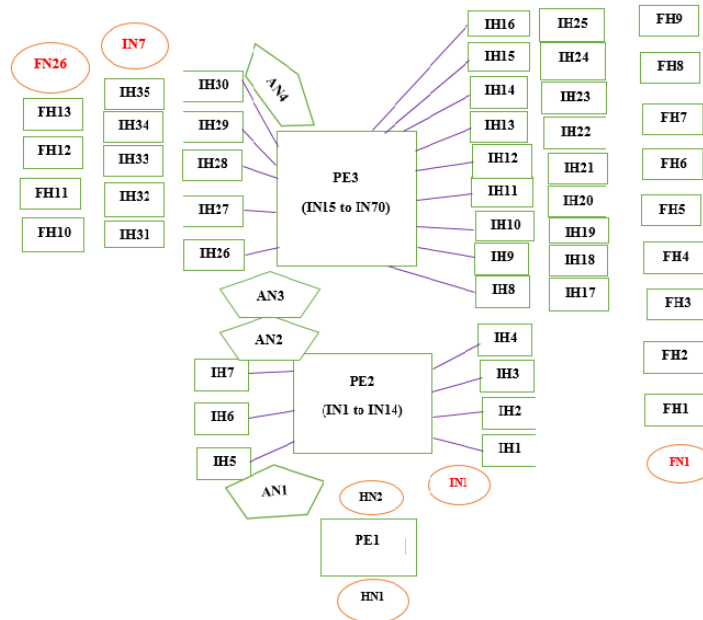


Fig. 5. Numbering system for 1D model at 20% of the span of the NGV

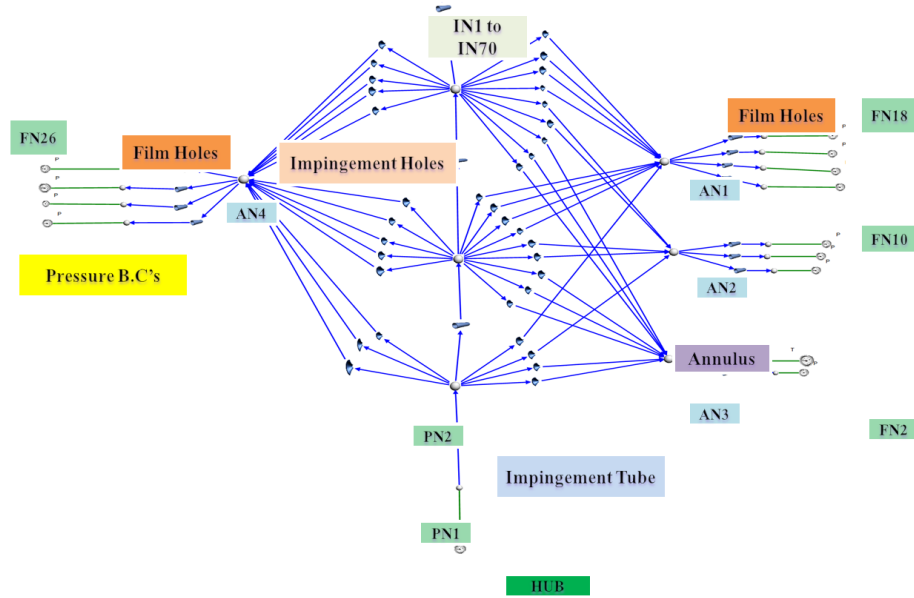


Fig. 6. Typical representation of Flow network model at 20% of the span of the NGV

### Application to NGV:

In the present study, a commercially available program Flownex code, which incorporates the 1D technique described above, is used for the analysis of flow and pressure distribution of the combined impingement and film hole of a typical gas turbine NGV.

Constituent elements of the NGV are represented into the one dimensional network model of the leading edge of a vane are as follows: The flow starts from the hub, and enters the impingement holes of the FIT. The PFH- film hole represented by 101 number of pipe elements numb; PFI: front impingement tube represented by 14 pipe elements and RIH: Impingement holes represented by 217 restrictors with respective discharge coefficients. A total of 179 nodes and 102 static pressure values taken from the CFD simulation are fed into the Network model. Similarly, the flow enters at AIT and then leaves at film holes through the impingement hole: PIH: Film hole represented by 55 pipe elements number, PFI: front impingement tube represented by 12 pipe elements and RIH: Impingement holes represented by 144 restrictors with discharge coefficients. Thus, a total of 64 nodes and 56 static pressure values taken from the CFD simulation are fed into the one network model.

Figure 6 shows a part of the final network representation of the NGV cooling passage from 0 (hub) to 20% span of the vane in Figure. 5. This section of the network contains (i) 2 numbers of the hub nodes (HN), (ii) 70 numbers of impingement hole nodes (IN), (iii) 4 numbers of annular nodes (AN) and (iv) 26 numbers of film hole nodes (FN). Nodes and elements other than

the first 20% of the total span are not shown for the sake of brevity and to avoid repetitions in Figure 6.

The inputs to the flow network model are (i) inlet coolant mass flow rate at the hub, (ii) inlet coolant temperature at the hub, (iii) coefficient of discharge calculated from CFD and (iv) exit static pressure values of film holes. The corresponding outputs of the FNM are (i) coolant mass flow rate at each impingement and film hole and (ii) pressure drop at each impingement and film hole respectively.

## 4. Results and discussion

### 4.1 Comparison of Pressure ratio distributions along the flow path

In order to validate the codes being used in the present work, the ‘flow testing’ results reported by

Jin et al.[7] for a typical film cooled first stage NGV of an aeroderivative turbine with a maximum pressure ratio of 1.5 across the flow path, are used as bench mark for comparison. The one- dimensional flow network approach has been applied to predict the secondary flow and pressure drop distribution. The predicted values of pressure ratios obtained from the Flownex<sup>®</sup> 8.6.1. 2642 code are compared with the experimental values in Fig.7. The experimentally measured values of the pressure ratio for the compressible flow across the third row film cooling holes on the pressure surface of the high pressure turbine blade [7] are shown by solid green rectangle. Present data agreed very well with the data, as shown by the green line. In addition, the results for SH4 and SH5 of the present geometry are also shown in the same

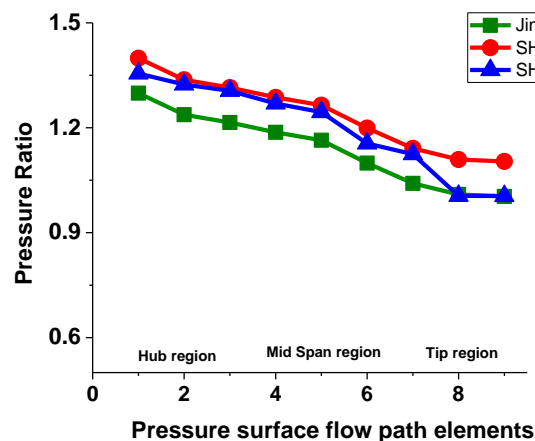


Fig. 7. Span wise pressure ratio distributions at the pressure surface of the vane

figure, with the same boundary conditions as in Jin [7]. The trends obtained in Fig.7 are similar to those in Jin [7].

## 4.2 Mass flow ate distribution

The minimum coolant requirement to the plenum of FIT for the combined impingement and film cooled NGV gemeotry was experimentally and numerically determined by Chandran and Prasad [16] to be 0.0035 kg/s. Taking this mass flow rate value as input, three dimensional analysis is carried out by FLUENT 14.5 to obtain discharge coefficients,  $C_d$ . These  $C_d$  values are inturn provided as input to the one-dimensional network model.

The coolant flow rate distribution at each jet impingement row of the holes on the outer surface of the FIT plenum channel, facing the leading edge, is shown in Fig. 8. Coolant air enters from the hub and rises towards the tip region of the leading edge circuit of the vane through FIT. Typically, these jet impingement mass flow rates are lower at the hub region, increase in the mid span region, but decrease in the tip region of the holes for all rows near leading edge. Such variations of impingement jet mass flow rates are a result of the crossflow momentum of the multiple jets as well as the jet deflection due to crossflow moment towards the downstream region of the flow path elements. The mass flow rates facing the suction surface of the vane indicated by inverted triangles with orange color through the jet impingement rows have much higher values due to higher deflection of the jets attained by their higher crossflow velocities. These effects are lower among the leading edge impingement rows. However, the sixth and twelfth elements of the IS1 row in the midspan region (facing suction surface, refer Fig.1) exhibit lower coolant jet mass flow rates because of insufficient jet crossflow momentum .

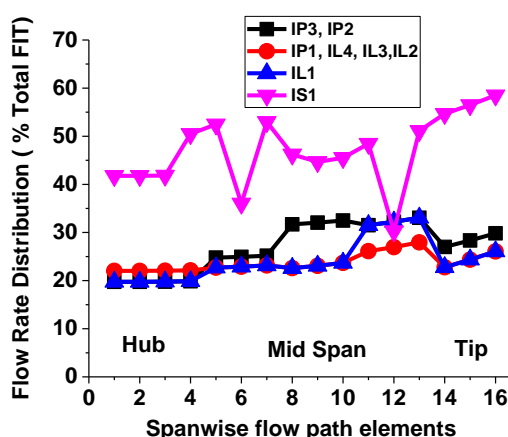


Fig. 8. Mass flow rate distribution at leading edge of the impingement holes

The percentage flow rates through the film holes SH1 to SH5 estimated from the network analysis are shown in Figure 9. As the coolant flow takes place from hub to tip (i.e from flow

path elements 1 to 9) there is a significant variation in the flow rates. For example, the flow rate at element 2 is the lowest and at element 3 is the highest for film holes SH1 and SH2 rows respectively. Similarly the mass flow rate at the element 6 is the lowest for the SH5 row. These results imply the possibility of high metal temperature near elements 2 and 6, while high thermal gradients may result near element 3. Remedial action such as providing material with stronger oxidation resistance is desirable in these regions.

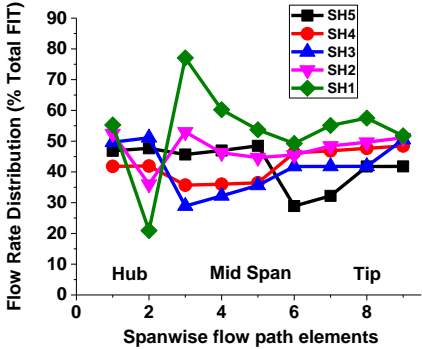


Fig. 9. Mass flow rate distribution at the leading edge of the film holes

Figure 10 shows a schematic representation of the percentage distribution of coolant from the FIT and AIT, which in turn flows out through the leading edge film holes, mid-chord zone and the trailing edge film holes. The coolant from FIT and AIT are 25.5% and 74.5% respectively. The secondary fluid flows from FIT is 24.3% fed to the leading edge film holes: SH1 to SH5 and SS1 and SS2. It is found that 51.9% of coolant is fed to the mid-chord region through the film holes in PS1 and PS2 rows and in SS3 and SS4 rows. The remaining 22.5% coolant flows out of the trailing edge film holes, namely the PS3 and PS4 row and the slot (not shown in Figure). Thus, Figure.10 provides the quantitative information about mass balance of all the outlets on the external surface of the vane.

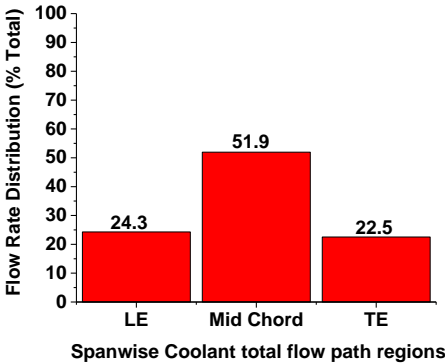


Fig. 10. Span wise total coolant flow rates at the leading edge region of the Film cooled rows

### 4.3 Pressure drops distribution at each row of the film holes

Figure 11 shows the pressure drop variation at leading edge of the impingement holes. The pressure drop is lower at the hub, increases in the mid span region and decreases at the tip. This behavior of pressure drop is action to the mass flow rate, in Fig.8, as expected. The lower pressure difference across the sixth jet impingement hole of the IS1 row is primarily due to insufficient crossflow momentum of the jets for the mass flow rate supplied in the plenum.

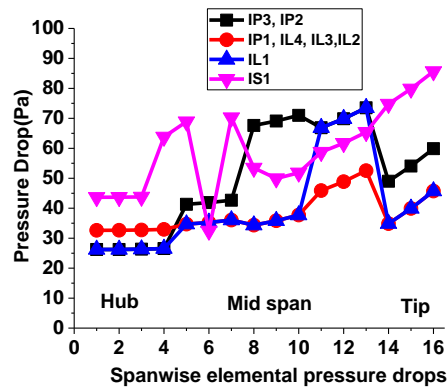


Fig. 11. Pressure drop variation at leading edge of the impingement holes

Figure 12 shows the span wise pressure drop variations at the leading edge of the film cooled rows. It is noticed that for a given minimum flow in the FIT plenum, along the flow path elements in the spanwise direction, minimum pressure drop occurs at second hole of the SH2 row, third hole of the SH3 row and sixth and seventh film cooling holes of the SH5 row. Although the values of pressure drop across these holes are much smaller, there is no danger of hot gas ingestion as they are all positive. The third hole of the SH1 row exhibits highest coolant pressure drop and hence corresponding high mass flow rate (refer Fig.9). This helps in the removal of more heat from the NGV surface and decreases the temperature of vane surface.

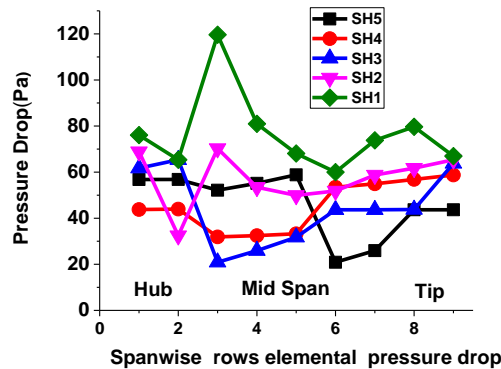


Fig. 12 Pressure drop variation at the leading edge of the film holes



## 4.4 Peripheral Variation

Mass flow rate and pressure drop distributions in the peripheral direction of the impingement holes of the leading edge circuit are shown in Figs. 13 and 14 respectively. It is observed that both flow rate and pressure drop are minimum in the holes of pressure surface region, decrease in the leading edge region holes and then drastically increase in the suction surface holes at various sectional planes. This phenomena is due to its higher jets crossflow momentum at the mid-cord region holes while these effects are smaller at the leading edge and tip region impingement holes.

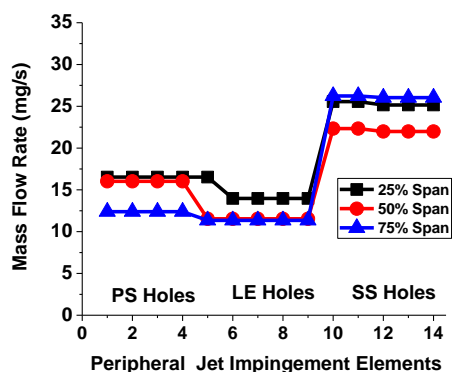


Fig. 13. Peripheral mass flow rate variation of the impingement holes

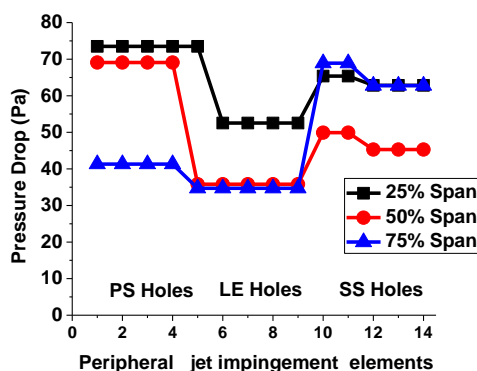


Fig. 14. Peripheral pressure drop variation of the jet impingement holes

## Conclusion

In the present work, coupled one dimensional flow network modeling and three-dimensional CFD approach for the efficient coolant flow distribution and as well as pressure drop at each row of the film cooling holes on the leading edge of the vane is demonstrated with

the help of film hole mass flow rate and hot gas ingestion for the combined impingement and film cooled first stage high pressure gas turbine NGV. The conclusions from this work are summarized as follows.

- The main advantages of one-dimensional flow network model with Flownex software is user-friendliness for modeling. The model is designed to perform flow and thermal analysis in a short turn around time and to permit sensitivity analysis for both varying fluid network structure and boundary conditions. Thus it is an effective tool in the analysis of cooled gas turbine NGV.

- The present vane is designed in such a way that the coolant flow rate at the leading edge lies between the flow rates from pressure and suction surfaces. Similar to the mass flow, the pressure drop near the leading edge of FIT lies between the values on the suction and pressure surfaces.

- The film holes with smaller values of the flow rates are responsible for increasing the NGV surface temperature. This may cause oxidation of material near the film hole, prompting to provide effective oxidation resistant material.

- The reduced coolant pressure drop at the film hole which affects the internal jet flow structure and in turn coolant inlet pressure decreases by the influence of the mainstream velocity and NGV surface temperature. This necessitate the reduction in life and durability of the cooled NGV.

- The Maximum discrepancy between the proposed approach and available literature values is within 5%, for the coolant mass flow rate and pressure drop variation at each row of the hole.

- Considering the variations of the mass flow rate and pressure it may be concluded that the temperature variations need to be carefully assessed for non-uniformities.

- The computations are performed on a DELL system, core-i5, 96GB RAM work station. The computational time taken for each simulation is approximately 4 days. But one-dimensional flow network model with Flownex software the computations are achieved only within 0.28 seconds for the same conditions. Hence modular nature of the network representation recommends for the parametric studies on the combined impingement and film cooled first stage NGV as the effects of different hole diameters, pitches, and its film hole row locations from the stagnation point etc, and can be easily carried out for efficient optimization of the cooled gas turbine vane. This is necessary to ensure the vane durability and life.

## References

1. W. P. Damerow, J. P. Murtaugh, F. Burggraf, Experimental and Analytical Investigation of the Coolant Flow Characteristics in Cooled Turbine Airfoils, 1972, NASA, USA, Tech. Paper, NASA-CR-120883.
2. H.F. Jen, J.B. Sobanik, Cooling Air Flow Characteristics in Gas Turbine Components, 1982, ASME Journal of Engineering for Power, vol. 104, pp. 275-280.
3. G.N. Kumar, R.J. Roelker, P.L. Meitner, A Generalized One-Dimensional Computer Code for Turbo machinery Cooling Passage Flow Calculations, 1989, NASA, USA, Tech Memo 102079, Technical Report 89-C-013, and also published at 25th Joint Propulsion Conference Monterey, CA, U.S.A .
4. C. Carcasci, B. Facchini, A Numerical Procedure to Design Internal Cooling of Gas Turbine Stator Blades, 1996, Revue Générale de Thermique, vol. 35, pp. 257.
5. T.J. Martin, G.S. Dulikravich, Analysis and multidisciplinary Optimization of internal coolant networks in turbine blades, 2002, AIAA Journal of propulsion and power, vol. 18, No. 4, pp. 896-906.
6. B.V.N. Rama Kumar, B.V.S.S.S. Prasad, A Combined CFD and Network Approach for a Simulated Turbine Blade Cooling System, 2006, Indian Journal of Engineering & Materials Sciences, vol. 13, pp. 195-201.
7. H. Jin, A. Riddle, L. Cooke, A Compressible Flow Network Analysis for Design Upgrade of Industrial Aero Derivative H. P Turbine Blades, 2008, presented at the ASME Turbo Expo, GT2008-50431, Berlin, Germany.
8. Z.R. Chi, W. Songtao, J. Ren, H.Jiang, Multi-Dimensional Platform for cooling Design of Air Cooled Turbine Blades, 2012, presented at the ASME Turbo Expo, GT2012-68675 Copenhagen, Denmark.
9. L. Andrei, A. Andreini, B. Facchini, L. Winchler, A decoupled CHT Procedure: application and validation on a gas turbine vane with different cooling configurations, 2013, Energy procedia, vol. 00, pp. 1-10.
10. P. Yan, Y. Curi, L. Shi, J. Zhu, Application of Conjugate Heat Transfer and Fluid Network Analysis to Improvement Design of Turbine Blade with Integrated Cooling Structures, 2013, Proc IMechE Part G: Journal of Aerospace Engineering, vol. 00, pp. 1-14.
11. L.V. Tran, and J.S. Kapat, Coupled Zero-Dimensional/One-Dimensional Model for Hybrid Heat Transfer Measurements, 2014, AIAA Journal of Thermophysics and Heat Transfer, vol. 28, pp. 236-250.
12. W. Che, S. Ding, C. Liu, A modeling method on aircraft engine based on the Component Method of secondary air system, 2014, Procedia Engineering, vol. 80, pp. 258 – 271.

13. A. Angersbach, D. Bestle, Optimization of Air Distribution in a Preliminary Design Stage of an Aero-Engine Combustor, 2014, 14th AIAA Aviation Technology, Integration, and Operations Conference, Atlanta, Georgia, USA, AIAA 2014-3004.
14. B. Suresh, A.B. Shivkumar., V. Kesavan, S. Kishore Kumar, Heat Transfer and Flow Studies of Different Cooling Configurations for Gas Turbine Rotor Blade, 2014, Proceedings of ASME Gas Turbine India conference, GTINDIA2014-8214, December 15-17, New Delhi, India.
15. N.H.K. Chowdhury, H. Zirakzadeh, J.C Han, A Predictive Model For Preliminary Gas Turbine Blade Cooling Analysis, 2015, Proceedings of ASME Turbo Expo GT2015-42205, June 15-19, Montréal, Canada.
16. D. Chandran, B. Prasad, Conjugate Heat Transfer Study of Combined Impingement and Showerhead Film Cooling Near NGV Leading Edge, 2015, International Journal of Rotating Machinery, Article ID: 315036.
17. G. Wang, Q. Gao, T. Zhang, Y. Wang, A simulation approach of under-hood thermal management, 2016, Advances in Engineering Software, vol. 100, pp. 43–52.
18. K.P. Reddy, B.V.S.S.S Prasad, Flow Analysis of Combined Impingement and Film Cooled Gas Turbine Nozzle Guide Vane, 2016, IEEE Aerospace Conference, Paper No: 2646, March, 5-12, Yellow Stone Conference Centre, Big Sky, Montana, USA.
19. F. Bavassano, M. Mantero, T. Gasnier, E. Ronconi, Analysis of Heavy Duty Gas Turbine Stator-Rotor Cavity through 3D CFD - 1D Fluid Network Field Measurements Combined Approach, 2016, Proceedings of ASME Turbo Expo, GT2016- 57629, June 13 – 17, 2016, Seoul, South Korea.

## Nomenclature

$\Delta p$	Pressure Drop (Pa)
$Tu$	Turbulence Intensity (%)
$\rho$	Density (kg/m <sup>3</sup> )
$h$	Specific Enthalpy ( J/Kg K)
$p$	Pressure (Pa)
$\dot{m}$	Mass flow rate (Kg/s)
$V$	Fluid Velocity (m/s)

K            loss Coefficient

Cd           Discharge Coefficient

Subscripts

i            inlet

e            exit

o            total